PROCEEDINGS OF SCIENCE

Search for critical point via intermittency analysis in NA61/SHINE

Tobiasz Czopowicz for the NA61/SHINE Collaboration
Jan Kochanowski University, Kielce
Warsaw University of Technology
E-mail: tobiasz.czopowicz@cern.ch

One of the main goals of NA61/SHINE, a fixed-target experiment at the CERN SPS, is the search for the critical point of strongly interacting matter. The comprehensive data collected during a two-dimensional scan in beam momentum (13A-150A GeV/c) and system size (p+p, p+Pb, Be+Be, Ar+Sc, Xe+La, Pb+Pb) allows, in particular, for a systematic search for an enhancement of fluctuations of various observables. An example of such observable is local fluctuation of particle densities in transverse momentum space, which can be probed with an intermittency analysis by measuring the scaling behavior of factorial moments of multiplicity distributions.
This contribution reviews the ongoing NA61/SHINE studies of scaled factorial moments of proton multiplicity distributions. New results were obtained for Ar+Sc at 150A GeV/c ($\sqrt{s_{NN}} \approx 17$ GeV) and Pb+Pb at 30A GeV/c ($\sqrt{s_{NN}} \approx 7.5$ GeV) collisions, employing a novel approach using cumulative quantities and independent data points are presented.

Critical Point and Onset of Deconfinement 2021
March 15-19, 2021
Online

PoS(CPOD2021)039

1. Introduction

Study of the phase diagram of the strongly interacting matter remains one of the main goals of theoretical and experimental research in heavy-ion physics. One of the key features of the diagram is the critical point – a hypothetical end-point of the first-order phase transition that has properties of the second-order phase transition [2, 3]. In the second-order phase transition, the correlation length diverges. The system becomes scale invariant, which leads to enhanced multiplicity fluctuations with special properties that can be revealed by scaled factorial moments.

Scaled factorial moments $F_r(M)$ of the order r are defined as:

$$F_r(M) = \frac{\left\langle \frac{1}{M}\sum_{i=1}^{M} n_i(n_i-1)\ldots(n_i-r+1) \right\rangle}{\left\langle \frac{1}{M}\sum_{i=1}^{M} n_i \right\rangle^r}, \tag{1.1}$$

where M is the number of 2-dimensional bins, n_i is the number of particles in i-th bin.

If the system is self-similar, factorial moments follow a power-law dependence on momentum bin width [4, 5, 6, 7]

$$F_r(M) \sim M^{\phi_r} \tag{1.2}$$

and, additionally, intermittency indices for different orders obey the linear relation

$$\phi_r = (r-1)\cdot d_r, \tag{1.3}$$

where the anomalous fractal dimension d_r is independent of r.

Theoretical expectations for ϕ_2 if a system freezes out at the QCD critical point, assuming that it belongs to 3D Ising universality class, is 5/6.

The idea was introduced by Bialas and Peschanski [6] in the late 80s. Some experimental results on the dependence of Scaled Factorial Moments of the multiplicity distribution on the momentum bin width have already been published. Two examples of such results are shown in Fig. 1. It shows $\Delta F_2(M)$ $(= F_2^{data}(M) - F_2^{mixed}(M))$ for mid-rapidity protons in central Si+Si at the top SPS energy from NA49 [12] and semi-central Ar+Sc from NA61/SHINE [13]. In both plots, a deviation from zero is observed and may be fitted with a power law. However, in both plots, the data points are correlated.

In this work, second scaled factorial moment dependence on the transverse momentum bin size for mid-rapidity protons produced in Ar+Sc at 150A GeV/c and Pb+Pb at 30A GeV/c collected by NA61/SHINE [1] using independent points and cumulative quantities will be presented.

2. Cumulative transformation

Scaled factorial moments strongly depend on the single-particle transverse momentum distribution that may dominate the possible effect of the critical point. There are two possible ways to minimize it. First, to construct mixed event data set by mixing particles from the recorded data such that each mixed event consists of particles from different true events. Then, calculate F_2^{mixed} and subtract from the original F_2^{data} to get ΔF_2.

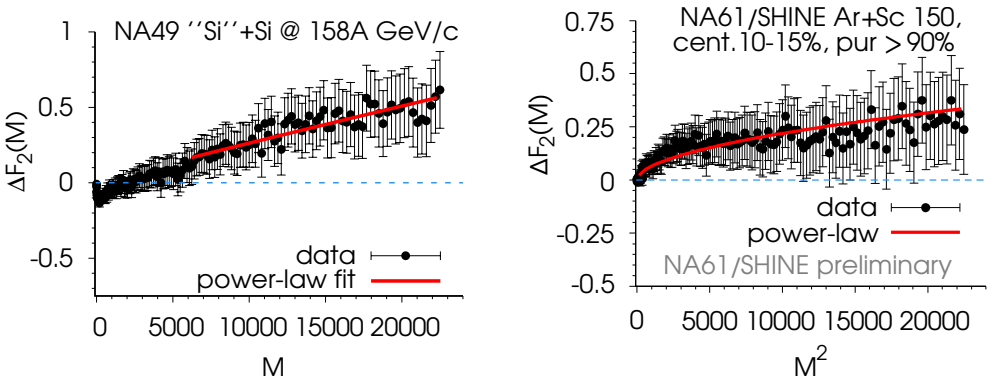

Figure 1: Second scaled factorial moment, ΔF_2, dependence on the number of transverse momentum bins M for mid-rapidity protons in central Si+Si at the top SPS energy from NA49 [12] (*left*) and semi-central Ar+Sc from NA61/SHINE [13] (*right*).

The other possibility is to transform transverse momentum components, p_x and p_y into their cumulative equivalents [14]. This transforms their distributions into uniform from 0 to 1 preserving (approximately) the power-law relation.

An example of the effect of the transformation is shown in Fig. 2. Initial transverse momentum components, p_x and p_y, have been transformed into their cumulative equivalents, Q_x and Q_y. As a result, their non-uniform distributions became uniform between 0 and 1.

3. Momentum-based Two-Track Distance cut

Time Projection Chambers, the main tracking devices at NA61/SHINE, are not able to distinguish between tracks that are too close to each other in space. At a small enough distance, their signals begin to overlap and seem to be one track with high energy loss. In order to compare experimental results with models (that do not have such limitation), a special cut had to be applied.

A momentum-based cut on two-track distance was introduced. It uses non standard momentum coordinates, i.e $s_x = p_x/p_{xz}$, $s_y = p_y/p_{xz}$ and $\rho = 1/p_{xz}$. For each data set, cut values were tuned by analyzing the mixed data set and comparing it to the recorded data. Then, the cut was applied to the data and all analyses models.

4. Results

Figure 3 presents the dependence of the second scaled factorial moments of mid-rapidity proton multiplicity distributions for 0-20% most central Ar+Sc at 150A GeV/c and 0-10% most central Pb+Pb at 30A GeV/c collisions. Each of the ten points is calculated using a fraction of the total available statistics, cumulative transverse momentum components were used and the momentum-based two-track distance cut was applied.

A separate analysis has shown that the momentum resolution of the detector may substantially distort the power-law form of $F_2(M)$. Therefore, $F_2(M)$ was analyzed in two ranges of momentum bin sizes, i.e. for M from 1 to 150 (Fig. 3, *top*) and from 1 to 32 (Fig. 3, *bottom*).

Clearly, no indication of a power-law increase with the number of bins is observed.

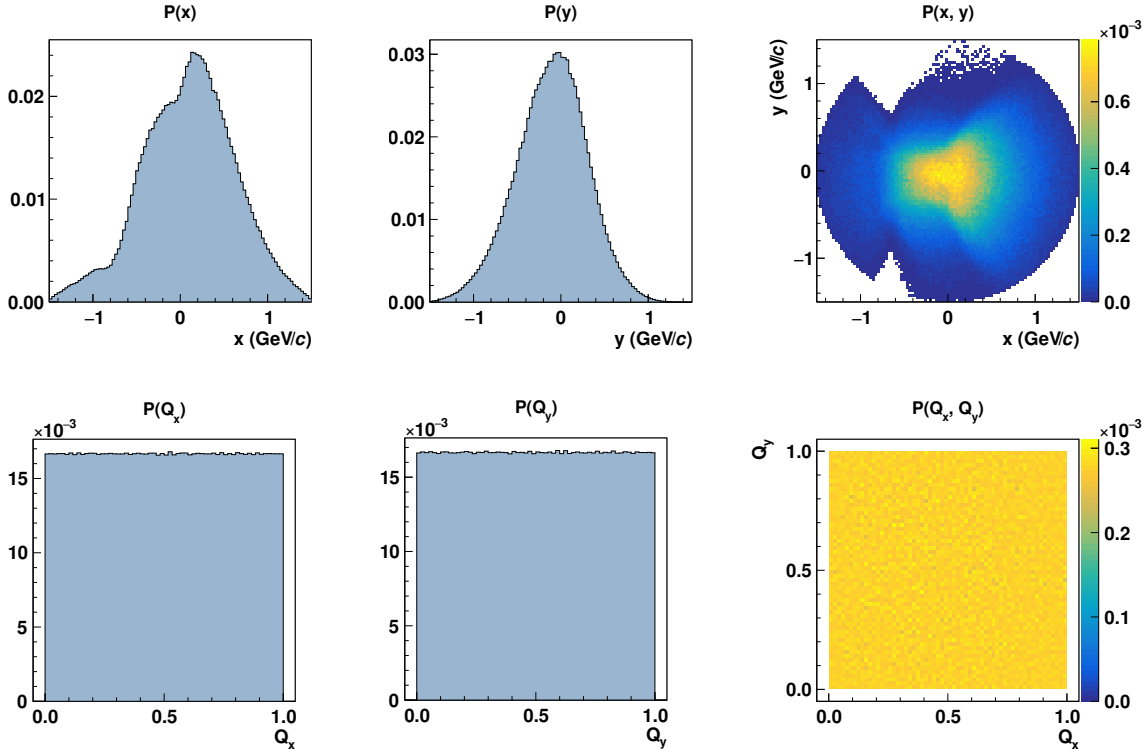

Figure 2: Example of the effect of the cumulative transformation of transverse momentum components, p_x and p_y, of proton candidates selected for intermittency analysis of NA61/SHINE Ar+Sc at 150A GeV/c data. Distributions before (*top*) and after (*bottom*) transformation.

5. Comparison with a model

A simple power-law model was introduced. It generates momenta of uncorrelated and correlated protons in events with a given multiplicity distribution. The model has two controllable parameters: the fraction of correlated particles and the strength of the correlation (the power-law exponent).

Using the model, lots of high statistics data sets with multiplicity distributions identical to the experimental data and similar inclusive transverse momentum distributions have been produced. Each of the data sets has a different fraction of correlated particles (varying from 0 to 4%) and/or different power-law exponent (varying from 0.0 to 1.0).

Next, all these generated data sets have been analyzed in the same way as the experimental data. $F_2(M)$ results have been compared and a p-value was calculated. An example of such comparisons is presented in Fig.4.

All p-values from each model data set, presented in one plot, form an *exclusion plot* (Fig. 5). The color scale is related to the probability that the model data set for a given number of correlated particles and a given power might be describing the data. White areas correspond to a p-value of less than 1% and may be considered excluded (for this particular model). The intermittency index ϕ_2 for a system freezing out at the QCD critical point is expected to be $\phi_2 = 5/6$ assuming that the latter belongs to the 3-D Ising universality class.

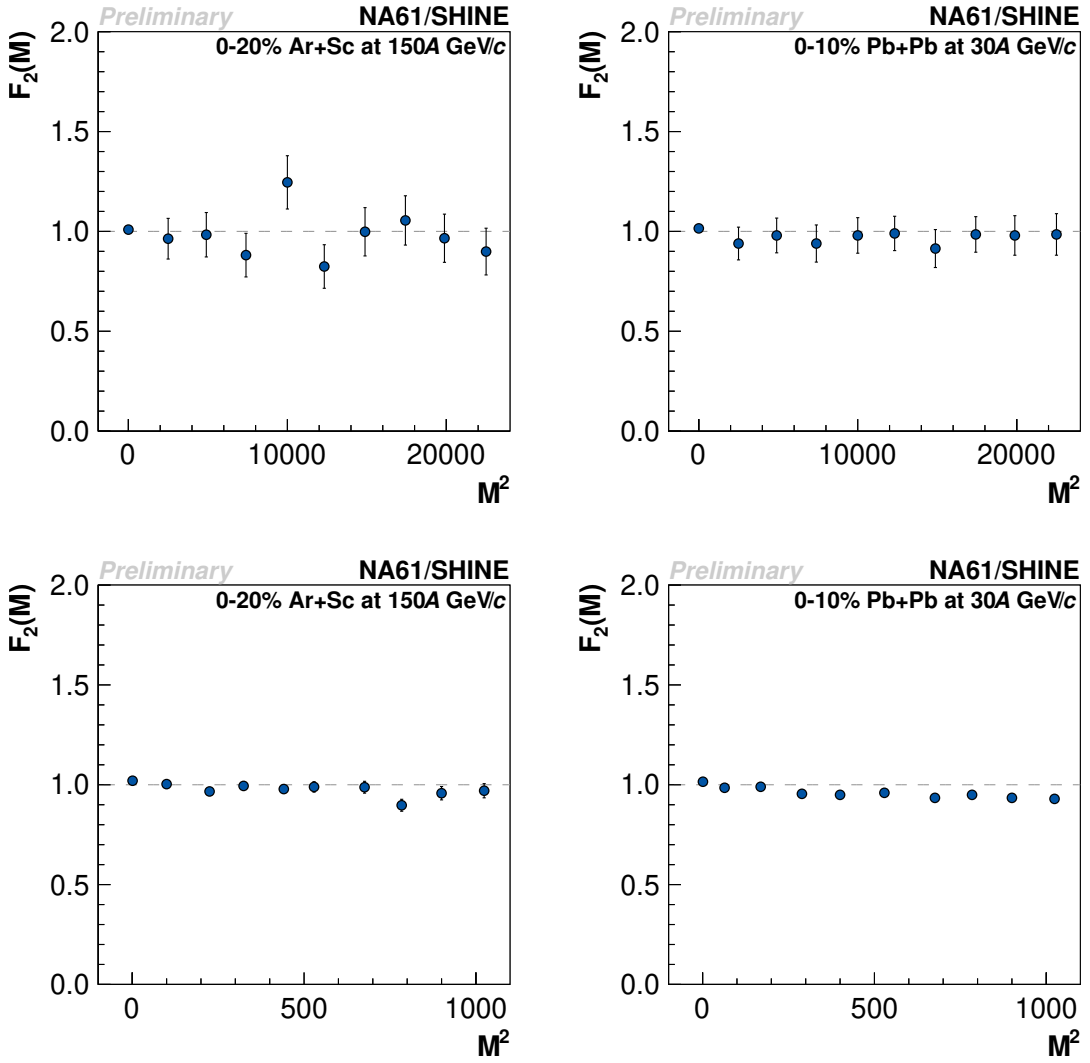

Figure 3: Results on the dependence of the second scaled factorial moment of the mid-rapidity proton multiplicity distributions for Ar+Sc at 150*A* GeV/*c* (*left*) and Pb+Pb at 30*A* GeV/*c* (*right*). Result obtained for M from 1 to 150 (*bottom*) and 1 to 32 (*top*). Only statistical uncertainties shown.

Even though the result on $F_2(M)$ is negative (no power-law increase observed), detailed comparison with a model can reveal excluded model parameters.

Acknowledgments

This work was supported by the Polish Ministry of Science and Higher Education (grant 2018/30/A/ST2/00226).

References

[1] N. Abgrall *et al.* [NA61], JINST **9** (2014), P06005

[2] M. Asakawa and K. Yazaki, Nucl. Phys. A **504**, 668 (1989).

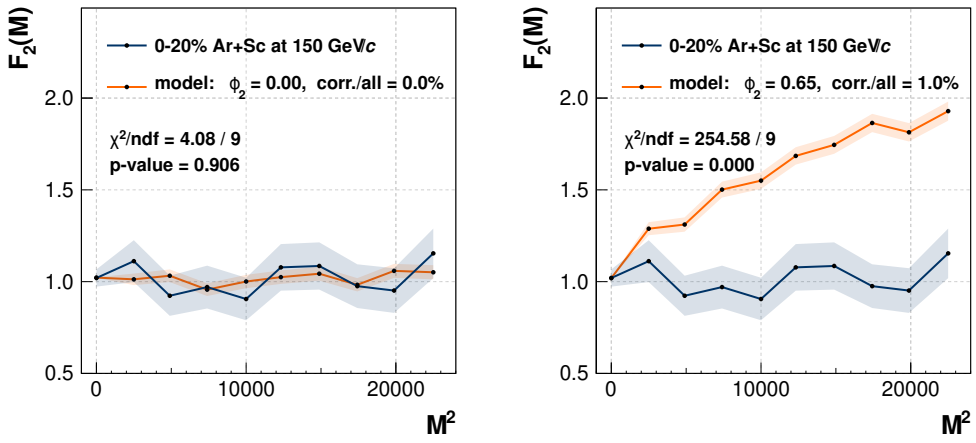

Figure 4: Example of the comparison of the simple power-law model data with experimental Ar+Sc at 150*A* GeV/*c*. No correlated particles (*left*) and 1% particles correlated with a power $\phi_2 = 0.65$ (*right*). Obtained χ^2 and p-value are used to construct the exclusion plot.

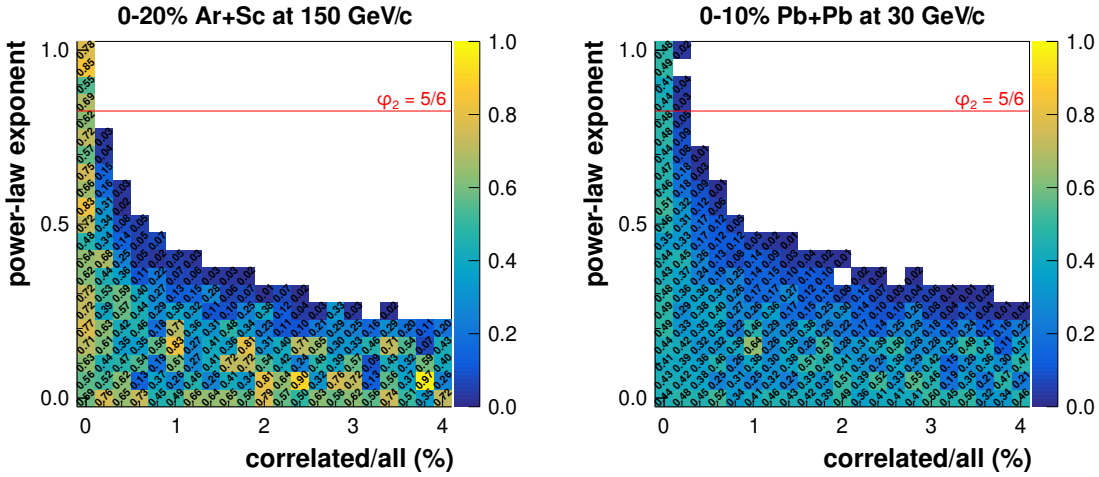

Figure 5: *Exclusion plots*: p-values for comparisons of $F_2(M)$ for Ar+Sc at 150*A* GeV/*c* (*left*) and Pb+Pb at 30*A* GeV/*c* (*right*) data with simple power-law model data sets with various values of two parameters (fraction of correlated particles and power-law exponent). White areas correspond to a p-value of less than 1%. Theoretical prediction for the power value for a system freezing out at the QCD critical point is marked with the red line.

[3] A. Barducci, R. Casalbuoni, S. De Curtis, R. Gatto and G. Pettini, Phys. Lett. B **231**, 463 (1989).

[4] J. Wosiek, Acta Phys. Polon. B**19**, 863 (1988).

[5] A. Bialas and R. C. Hwa, Phys. Lett. B **253**, 436 (1991).

[6] A. Bialas and R. B. Peschanski, Nucl. Phys. B **273**, 703 (1986).

[7] N. G. Antoniou, F. K. Diakonos, A. S. Kapoyannis and K. S. Kousouris, Phys. Rev. Lett. **97**, 032002 (2006).

[8] K. J. Sun, L. W. Chen, C. M. Ko and Z. Xu, Phys. Lett. B **774**, 103 (2017).

[9] E. Shuryak and J. Torres-Rincon, Nucl. Phys. A **982**, 831 (2019).

[10] M. Gazdzicki [NA61/SHINE Collaboration], PoS CPOD **2017**, 012 (2018).

[11] E. Andronov [NA61/SHINE Collaboration], Acta Phys. Polon. Supp. **10** 449 (2017).

[12] T. Anticic *et al.* [NA49 Collaboration], Eur. Phys. J. C **75**, no. 12, 587 (2015).

[13] N. Davis [NA61/SHINE], Acta Phys. Polon. Supp. **13**, no.4, 637-643 (2020)

[14] A. Bialas and M. Gazdzicki, Phys. Lett. B **252** (1990), 483-486